Stem Cell Reports, Volume *9*

Supplemental Information

An Efficient Platform for Astrocyte Differentiation from Human Induced Pluripotent Stem Cells

Julia TCW, Minghui Wang, Anna A. Pimenova, Kathryn R. Bowles, Brigham J. Hartley, Emre Lacin, Saima I. Machlovi, Rawan Abdelaal, Celeste M. Karch, Hemali Phatnani, Paul A. Slesinger, Bin Zhang, Alison M. Goate, and Kristen J. Brennand

SUPPLEMENTARY INFORMATION

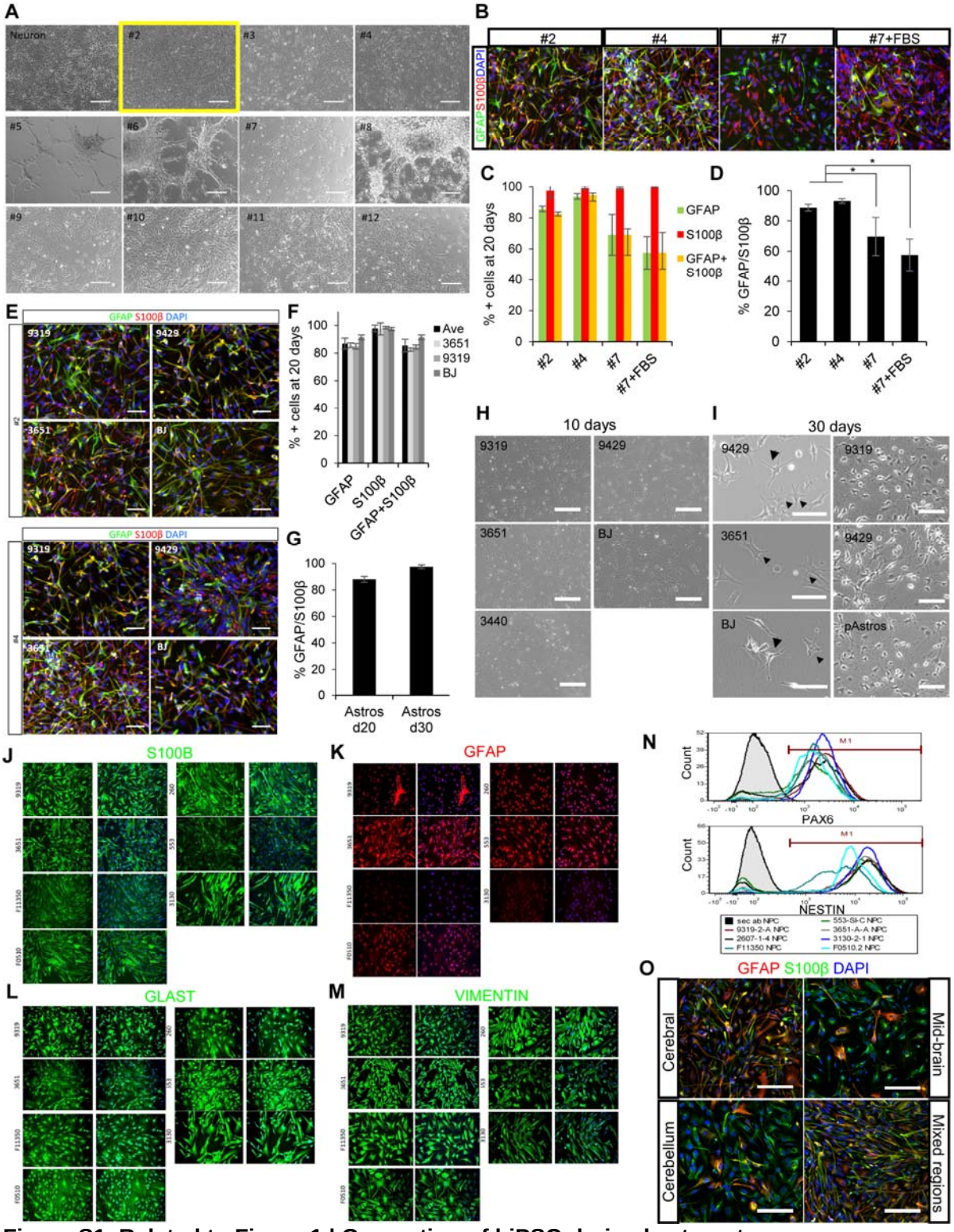

Figure S1. Related to Figure 1 | Generation of hiPSC-derived astrocytes.

(**A**) Cell morphologies across 12 screening conditions including 11 astrocyte differentiation condition and 1 cortical neuron differentiation condition after 20 days of differentiation from

NPCs. (**B**) Representative images of GFAP (green) and S100β (red) positive cells from two cell lines in top four selected conditions from (**A**). (**C**) Quantification of the number of cells positive for GFAP and S100β protein (N=5 from two cell lines) in top four selected conditions from (**A**). (**D**) Quantification of GFAP-positive cells normalized by S100β-positive cells (N=5 from two cell lines in top four selected conditions from (**A**). (**E**) Representative immunofluorescence images of GFAP (green) and S100β (red) across hiPSC-astrocytes differentiated from four control NPC lines (**Table S2**) at 20 days of differentiation using medium #2 condition. Images are quantified in (**F**) and (**G**). (**F**) Quantification of the number of cells positive for GFAP and S100β across hiPSC-astrocytes differentiated from four control NPC lines at 20 days of differentiation using medium #2 condition. (**G**) Percentage of GFAP-positive cells normalized by S100β-positive cells at 20 days and 30 days of differentiation using medium #2 condition. (**H**) Bright field images of hiPSC-astrocytes differentiated from 5 control NPC lines (**Table S2**) showing a similar astrocyte morphology at 10 days after medium #2 exposure. Scale bar = 500 µm. (**I**) Bright field images of hiPSC-astrocytes differentiated from 5 control NPC lines (**Table S2**) at 30 days of differentiation. Arrows represent fibrous-like morphology and arrowheads represent protoplasmic-like morphology of astrocytes. Each cell line includes both shapes of astrocytes (left, Scale bar = 200 µm). Higher density culture displays star-shaped astrocyte morphology (right, Scale bar = 500 µm). (**J-M**) Representative immunofluorescence images of S100β (green), GFAP (red), GLAST (EAAT1) (green) and VIMENTIN (green) of hiPSC-astrocytes differentiated from 7 control NPC lines from three independent hiPSC cohorts (**Table S2**). Scale bar = 200 µm. (**N**) Flow cytometric analysis of PAX6 and NESTIN-positive cells from the 7 isogenic NPC lines used for hiPSC-astrocyte differentiations in **J-M**. M1 represents positive cells expressing each marker protein. (**O**) GFAP (red) and S100β (green)-staining in primary astrocytes from different regions of human fetal brain including cerebral cortex, mid-brain, cerebellum and the whole brain (labeled mixed regions). Scale bar = 200 µm. Data are represented as mean ± error bar (Standard Deviation). hiPSC-Astros: human hiPSC-derived astrocytes, pAstros: primary human fetal astrocytes. A two-tailed homoscedastic Student's t-test, n.s.: not significant, * $p < 0.05$, ** $p < 0.01$, *** $p < 0.001$.

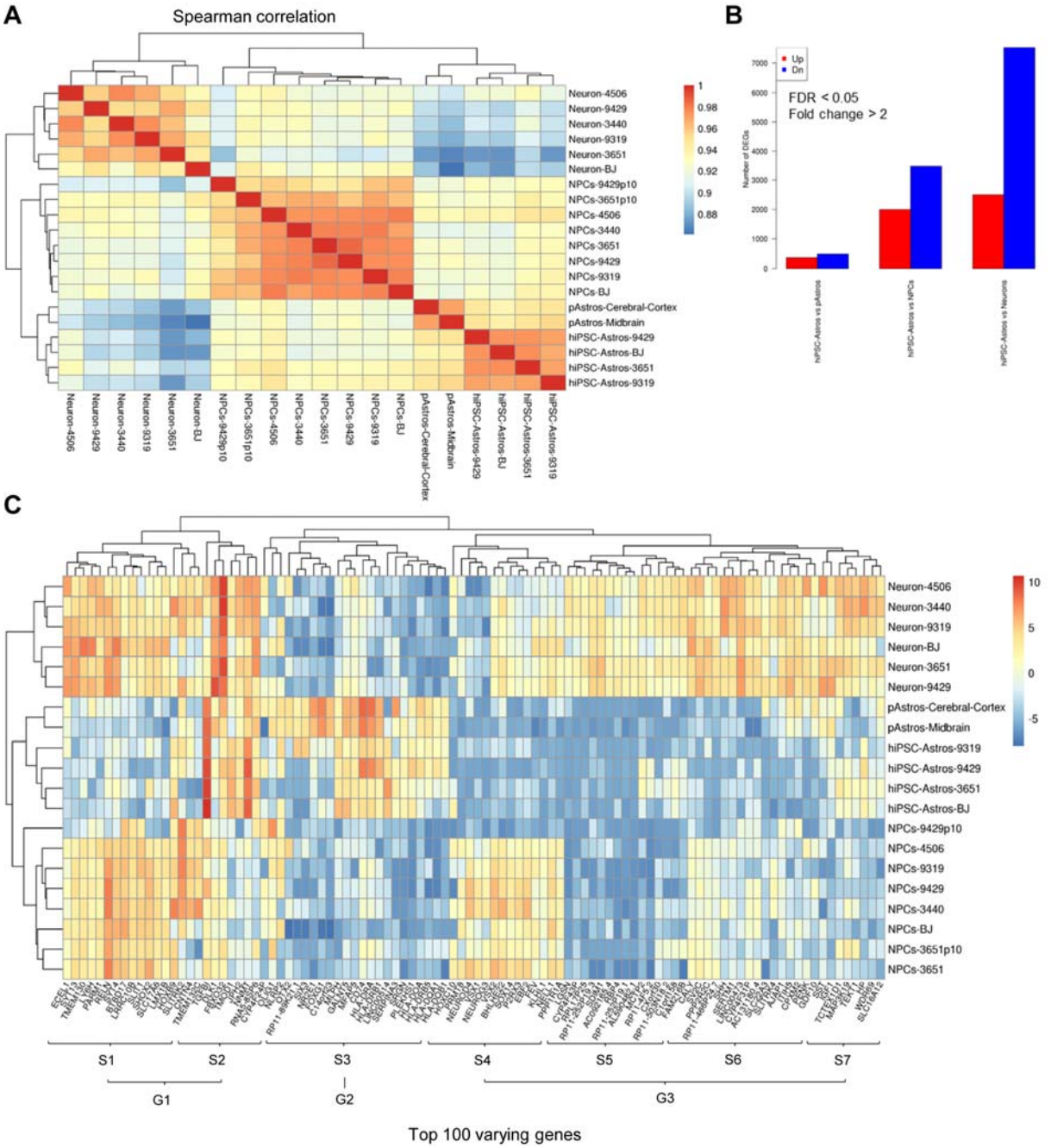

Figure S2. Related to Figure 2 | Global gene expression profiling to compare the transcriptional profile of hiPSC-derived astrocytes and primary human fetal astrocytes.
RNAseq analysis of hiPSC-derived NPCs (N=8), neurons (N=6) and astrocytes (N=4) together with pAstrocytes (N=2) from the cerebral cortex and midbrain region. (**A**) Spearman correlation analysis of hiPSC-derived NPCs, neurons and astrocytes, together with pAstrocytes. (**B**) The number of genes differentially expressed between hiPSC-astrocytes and pAstrocytes, as well as between hiPSC-astrocytes and hiPSC-derived NPCs or neurons: less than 400 genes were differentially expressed (upregulated or downregulated, respectively) in hiPSC-astrocytes relative to pAstrocytes, while nearly 10,000 genes were differentially expressed between hiPSC-astrocytes and hiPSC-neurons. hiPSC-Astros: hiPSC-astrocytes, pAstros: primary astrocytes.

(**C**) Heatmap of hiPSC-derived NPCs, neurons and astrocytes compared to fetal and adult brain tissue (GSE73721) (Zhang et al., 2016) using the top 100 most varying genes, clustered by group (G) 1-3 and sub-group (S) 1-7.

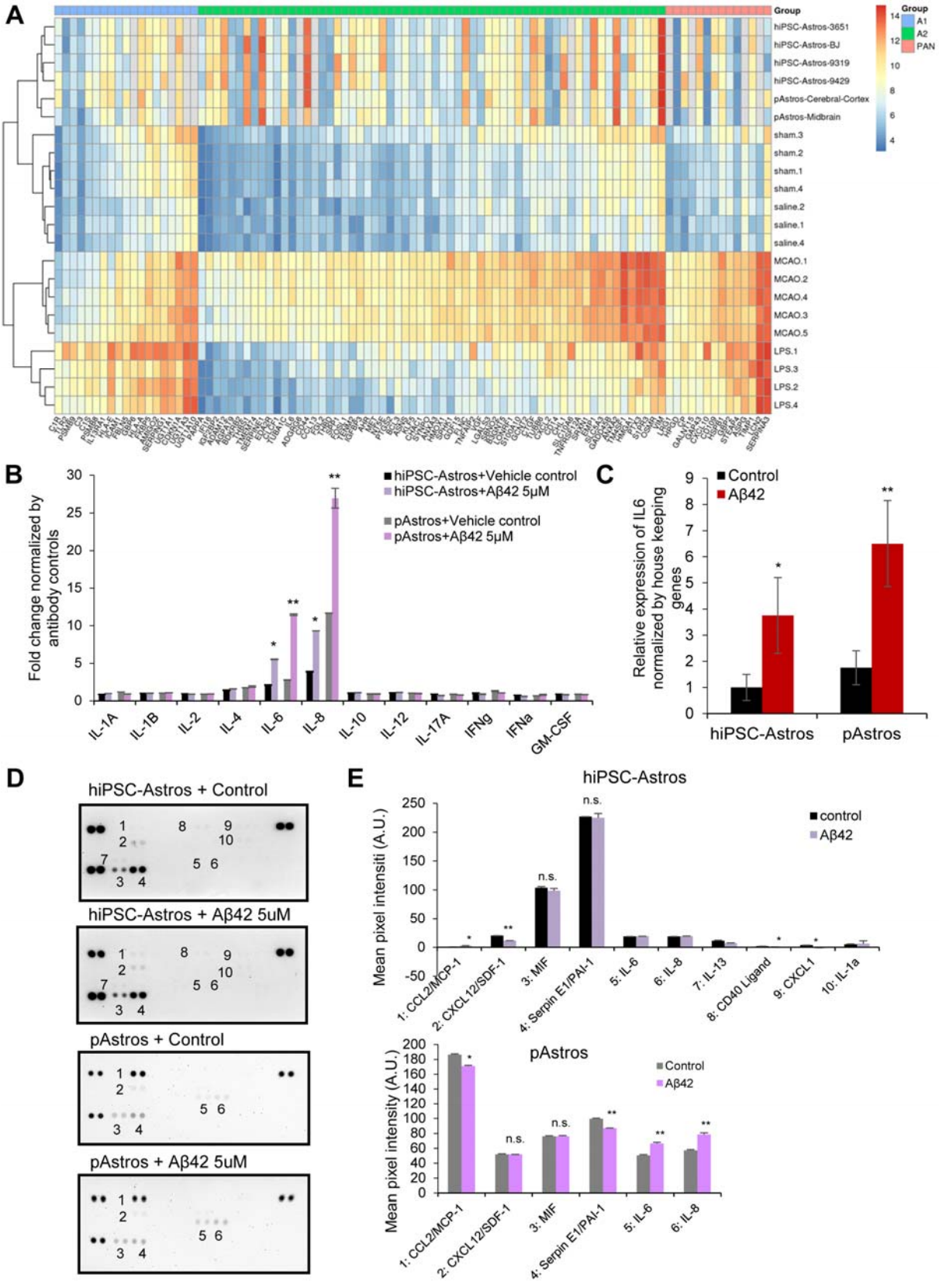
A
Group
hiPSC-Astros-3651
hiPSC-Astros-BJ
hiPSC-Astros-9319
hiPSC-Astros-9429
pAstros-Cerebral-Cortex
pAstros-Midbrain
sham.3
sham.2
sham.1
sham.4
saline.2
saline.1
saline.4
MCAO.1
MCAO.2
MCAO.4
MCAO.3
MCAO.5
LPS.1
LPS.3
LPS.2
LPS.4
Group
A1
A2
PAN
14
12
10
8
6
4
B
Fold change normalized by antibody controls
hiPSC-Astros+Vehicle control
hiPSC-Astros+Aβ42 5μM
pAstros+Vehicle control
pAstros+Aβ42 5μM
IL-1A
IL-1B
IL-2
IL-4
IL-6
IL-8
IL-10
IL-12
IL-17A
IFNg
IFNa
GM-CSF
C
Relative expression of IL6 normalized by house keeping genes
Control
Aβ42
hiPSC-Astros
pAstros
D
hiPSC-Astros + Control
hiPSC-Astros + Aβ42 5uM
pAstros + Control
pAstros + Aβ42 5uM
E
hiPSC-Astros
Mean pixel intensiti (A.U.)
control
Aβ42
1: CCL2/MCP-1
2: CXCL12/SDF-1
3: MIF
4: Serpin E1/PAI-1
5: IL-6
6: IL-8
7: IL-13
8: CD40 Ligand
9: CXCL1
10: IL-1a
pAstros
Mean pixel intensity (A.U.)
Control
Aβ42

Figure S3. Related to Figure 3 | Characterization of the neuroinflammatory status and reactivity of hiPSC-astrocytes.

(**A**) Heatmap-based cluster analysis of hiPSC-astrocytes and pAstrocytes compared to the astrocyte reactivity dataset (Zamanian et al., 2012), which was sorted by reactivity genes enriched in the A1 (LPS-treatment), A2 (MCAO ischemia) and pan-reactive phenotypes, or related controls (saline and sham, respectively). (**B**) Cytokine secretion from hiPSC-astrocytes and pAstrocytes measured by ELISA in response to 24-hour treatment with 5 μM Aβ42. (N=2 from two different hiPSC-astrocyte lines and two independent preparations of pAstrocytes cerebral cortex, N, independent experiments.) (**C**) *IL-6* gene expression changes in samples used for (**D**). (N=3 from two different hiPSC-astrocyte lines and two independent preparations of pAstrocytes cerebral cortex, N, independent experiments.) (**D**) Proteome profiler human cytokine array (targets are listed in **Table S4**) of hiPSC-astrocytes and pAstrocytes, with or without 5 μM Aβ42 treatment. Unlabeled dot blots are positive experimental controls from the manufacturer. (**E**) Quantification of dot blots in (**D**). (N=2 from two different hiPSC-astrocyte lines and two independent preparations of pAstrocytes cerebral cortex, N, independent experiments.) Proteome profiler human cytokine array tests chemokine levels. Data are represented as mean ± SD. hiPSC-Astros: hiPSC-derived astrocytes, pAstros: primary astrocytes. A two-tailed homoscedastic Student's t-test, n.s.: not significant, * $p < 0.05$, ** $p < 0.01$, *** $p < 0.001$

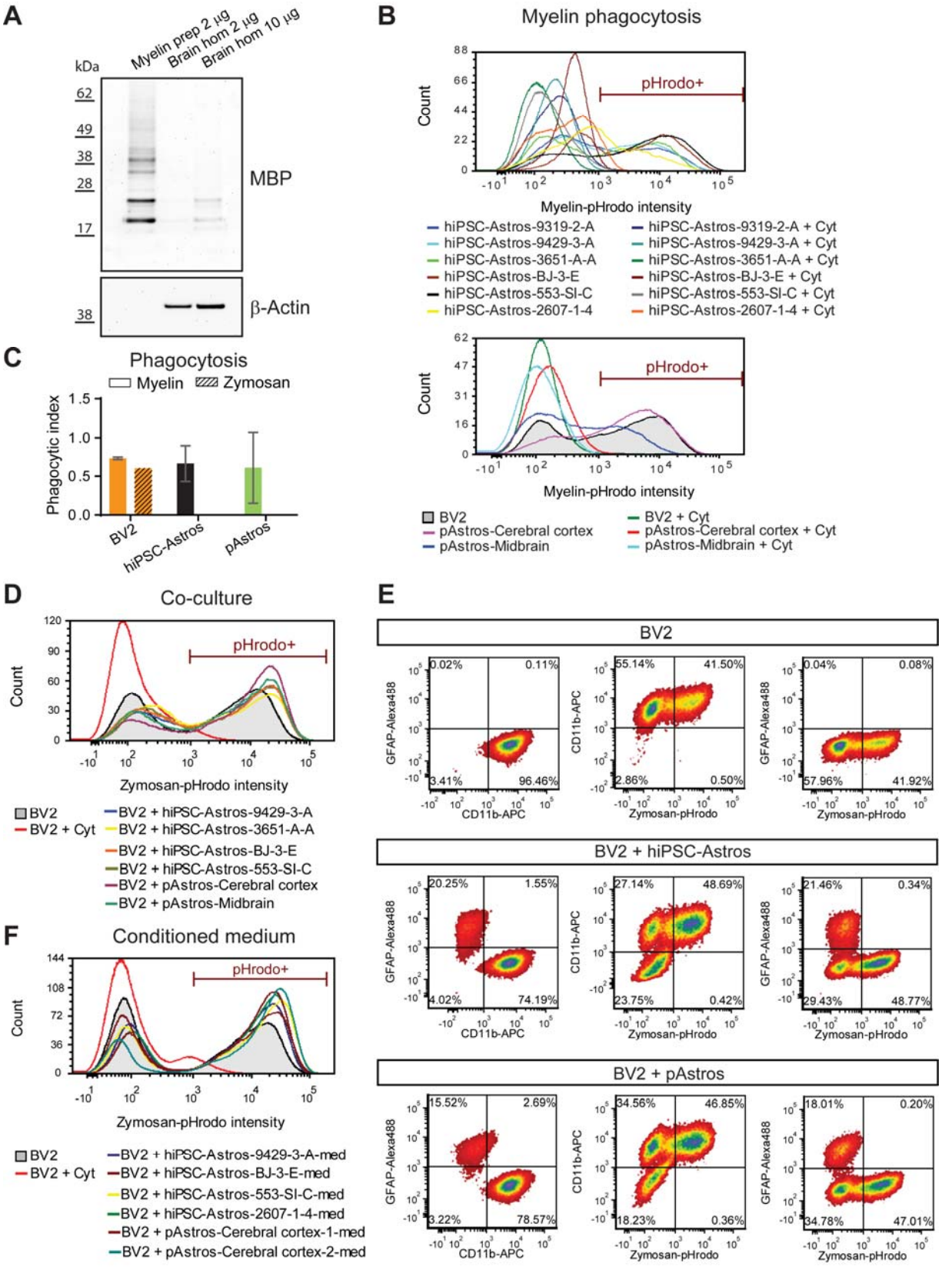
A
Myelin prep 2 µg
Brain hom 2 µg
Brain hom 10 µg
kDa
62
49
38
28
17
MBP
38
β-Actin
B
Myelin phagocytosis
Count
pHrodo+
Myelin-pHrodo intensity
hiPSC-Astros-9319-2-A
hiPSC-Astros-9429-3-A
hiPSC-Astros-3651-A-A
hiPSC-Astros-BJ-3-E
hiPSC-Astros-553-SI-C
hiPSC-Astros-2607-1-4
hiPSC-Astros-9319-2-A + Cyt
hiPSC-Astros-9429-3-A + Cyt
hiPSC-Astros-3651-A-A + Cyt
hiPSC-Astros-BJ-3-E + Cyt
hiPSC-Astros-553-SI-C + Cyt
hiPSC-Astros-2607-1-4 + Cyt
BV2
pAstros-Cerebral cortex
pAstros-Midbrain
BV2 + Cyt
pAstros-Cerebral cortex + Cyt
pAstros-Midbrain + Cyt
C
Phagocytosis
Myelin
Zymosan
Phagocytic index
BV2
hiPSC-Astros
pAstros
D
Co-culture
Zymosan-pHrodo intensity
BV2
BV2 + Cyt
BV2 + hiPSC-Astros-9429-3-A
BV2 + hiPSC-Astros-3651-A-A
BV2 + hiPSC-Astros-BJ-3-E
BV2 + hiPSC-Astros-553-SI-C
BV2 + pAstros-Cerebral cortex
BV2 + pAstros-Midbrain
E
BV2
BV2 + hiPSC-Astros
BV2 + pAstros
GFAP-Alexa488
CD11b-APC
Zymosan-pHrodo
0.02%
0.11%
3.41%
96.46%
55.14%
41.50%
2.86%
0.50%
0.04%
0.08%
57.96%
41.92%
20.25%
1.55%
4.02%
74.19%
27.14%
48.69%
23.75%
0.42%
21.46%
0.34%
29.43%
48.77%
15.52%
2.69%
3.22%
78.57%
34.56%
46.85%
18.23%
0.36%
18.01%
0.20%
34.78%
47.01%
F
Conditioned medium
Zymosan-pHrodo intensity
BV2
BV2 + Cyt
BV2 + hiPSC-Astros-9429-3-A-med
BV2 + hiPSC-Astros-BJ-3-E-med
BV2 + hiPSC-Astros-553-SI-C-med
BV2 + hiPSC-Astros-2607-1-4-med
BV2 + pAstros-Cerebral cortex-1-med
BV2 + pAstros-Cerebral cortex-2-med

Figure S4. Related to Figure 4 | Impact of hiPSC-astrocytes on the phagocytic ability of BV2 microglial cells.

(**A**) Myelin is enriched after purification from brain (myelin prep) compared to whole brain homogenate (brain hom) as detected by western blotting. (**B, D, F**) Representative histograms used to quantify the values displayed in **Figure 4A, 4C, 4D** are shown in (**B**, **D**, **F**), respectively. Phagocytosing cells are marked as pHrodo+. (**C**) Phagocytic indices of BV2 cells, hiPSC-astrocytes and pAstrocytes incubated with 20 μg of pHrodo-labeled myelin or zymosan for 3 hours and analyzed by flow cytometry. Values were averaged from 4 to 8 different control hiPSC-Astrocytes and 2 to 4 different pAstrocytes. (**E**) Flow cytometry analysis of BV2 microglial cells and co-cultures of hiPSC-astrocytes and pAstrocytes with BV2 microglial cells stained with CD11b-APC and GFAP antibodies (n=5). Representative fluorescent intensity dot plots are shown. Data are representative of three independent experiments (n = 3) and shown as mean ± standard deviation. Treatment with 2 μM Cytochalasin D (Cyt) was used as a negative control for phagocytosis inhibition.

Table S1 | Screening results for the 11 initial astrocyte differentiation conditions.

Medium	Cell line	TUJ1	MAP2	GFAP	S100B	Cell condition and morphology	Subjective score for astrocyte differentiation
#1. Neuron	3651	+	+	-	-	Neuronal morphology	N.A
	4506	+	+	-	-		
#2. ScienCell	3651	+	-	+	+	Highly proliferative Astrocyte morphology	+++
	4506	+	-	+	+		
#3. Gibco	3651	+	-	-	-	Highly proliferative Resemble fibroblasts	-
	4506	+	+	+	+		
#4. Lonza	3651	+	-	+	+	Highly proliferative Astrocyte morphology	+++
	4506	+	-	+	+		
#5.	3651	+	-	+	+	Not proliferative Form spheres	+
	4506	+	-	+	+		
#6.	3651	+	-	-	-	Not proliferative Cell line variation	-
	4506	+	-	+	+		
#7.	3651	+	-	+	+	Not proliferative Astrocyte morphology	++
	4506	+	+	+	+		
#8.	3651	+	+	-	-	Cell death Not proliferative	-
	4506	+		+	+		
#9.	3651	+	-	-	-	Not proliferative Cell line variation	-
	4506	+		-	+		
#10.	3651	+	-	-	-	Cell line variation	+
	4506	+	+	-	+		
#11.	3651	+	-	+	+	Cell line variation	+
	4506	+	+	-	+		
#12.	3651	+	-	-	-	No astrocyte markers presence	-
	4506	+	+	-	-		

#1 is cortical neuron differentiation control and #2-12 are astrocyte differentiation conditions. Screening results from two cell lines evaluated by staining with a neuronal lineage marker, Class III β-tubulin (TUJ1), a neuronal marker, MAP2, astrocyte markers, GFAP and S100B, cell survival conditions and astrocyte-like morphologies.

Table S2 | Cell lines tested in each essay by four investigators.

			Astrocyte										NPC									
Cell line	Donor Sex	Grown by	IF		qRTPCR		FACS		IL-6 ELISA		RNAseq		IF		qRTPCR		FACS		IL-6 ELISA		RNAseq	
pAst Ctx	F	INV1	✓	INV3	✓	INV3	✓	INV4	✓	INV1	✓	INV1	N/A		N/A		N/A		N/A		N/A	
pAst Mb	M	INV1	✓	INV3	✓	INV3	✓	INV4	✓	INV1	✓	INV1	N/A		N/A		N/A		N/A		N/A	
pAst Cblm	F	INV1	✓	INV3	✓	INV3	✓	INV4	✓	INV1	✓	INV1	N/A		N/A		N/A		N/A		N/A	
pAst Mix	Unknown	INV1	✓	INV3	✓	INV3	✓	INV4	✓	INV1	x		N/A		N/A		N/A		N/A		N/A	
Total # of lines tested per assay			4		4		4		4		3											
9319-2-A	F	INV1	✓	INV1	✓	INV1	✓	INV4	✓	INV1	✓	INV1	✓	INV1	✓	INV1	✓	INV4	x		✓	INV1
3651-A-A	F	INV1	✓	INV1	✓	INV1	✓	INV4	✓	INV1	✓	INV1	✓	INV1	✓	INV1	✓	INV4	x		✓	INV1
9429-3-A	F	INV1	✓	INV1	✓	INV1	✓	INV4	✓	INV1	✓	INV1	✓	INV1	✓	INV1	✓	INV4	x		✓	INV1
BJ-3-E	M	INV1	✓	INV1	✓	INV1	✓	INV4	✓	INV1	✓	INV1	✓	INV1	✓	INV1	✓	INV4	x		✓	INV1
9319-2-A (2)	F	INV1	✓	INV1, 3	✓	INV1, 3	✓	INV4	✓	INV1	x		✓	INV1, 3	✓	INV1, 3	✓	INV4	✓	INV1	x	
3651-A-A (2)	F	INV1	✓	INV1, 3	✓	INV1, 3	✓	INV1	✓	INV1	x		✓	INV1, 3	✓	INV1, 3	✓	INV4	✓	INV1	✓	INV1
9429-3-A (2)	F	INV1	✓	INV1	✓	INV1	✓	INV1	✓	INV1	x		✓	INV1	✓	INV1	✓	INV4	x		✓	INV1
BJ-3-E (2)	M	INV1	✓	INV1	✓	INV1	✓	INV4	✓	INV1	x		✓	INV1	✓	INV1	✓	INV4	x		x	
F11350	M	INV3	✓	INV3	✓	INV3	✓	INV4	✓	INV1	x		✓	INV3	✓	INV3	✓	INV4	x		x	
F0510	M	INV3	✓	INV3	✓	INV3	✓	INV4	✓	INV1	x		✓	INV3	✓	INV3	✓	INV4	x		x	
2607-1-4	M	INV1	✓	INV3	✓	INV3	✓	INV4	✓	INV1	x		✓	INV3	✓	INV3	✓	INV4	x		x	
553-SI-C	M	INV1	✓	INV3	✓	INV3	✓	INV4	✓	INV1	x		✓	INV3	✓	INV3	✓	INV4	x		x	
3130-2-1	M	INV1	✓	INV3	✓	INV3	✓	INV4	✓	INV1	x		✓	INV3	✓	INV3	✓	INV4	x		x	
3113-3-2	F	INV1	x		x		✓	INV1	x		x		x		x		x		x		x	
3183-1-9	F	INV1	x		x		✓	INV1	x		x		x		x		x		x		x	
690-1-4	M	INV1	x		x		✓	INV1	x		x		x		x		x		x		x	
676-1-2	F	INV1	x		x		✓	INV1	x		x		x		x		x		x		x	
1442-4-3	M	INV1	x		x		✓	INV1	x		x		x		x		x		x		x	
2011-3-2	F	INV1	x		x		✓	INV1	x		x		x		x		x		x		x	
2620-B-4	M	INV1	x		x		✓	INV1	x		x		x		x		x		x		x	
2607-1-4 (2)	M	INV2	x		✓	INV3	✓	INV2	x		x		x		✓	INV3	x		x		x	
553-SI-C (2)	M	INV2	x		✓	INV3	✓	INV2	x		x		x		✓	INV3	x		x		x	
3113-3-2 (2)	F	INV2	x		✓	INV3	✓	INV2	x		x		x		✓	INV3	x		x		x	
690-1-4 (2)	M	INV2	x		✓	INV3	✓	INV2	x		x		x		✓	INV3	x		x		x	
676-1-2 (2)	F	INV2	x		x		✓	INV2	x		x		x		x		x		x		x	
1442-4-3 (2)	M	INV2	x		✓	INV3	✓	INV2	x		x		x		✓	INV3	x		x		x	
2620-B-4 (2)	M	INV2	x		✓	INV3	✓	INV2	x		x		x		✓	INV3	x		x		x	
2011-3-2 (2)	F	INV2	x		x		✓	INV2	x		x		x		x		x		x		x	
3130-2-3	M	INV2	x		✓	INV3	✓	INV2	x		x		x		✓	INV3	x		x		x	
499-5-2	M	INV2	x		x		✓	INV2	x		x		x		x		x		x		x	
581-1-2	M	INV2	x		✓	INV3	✓	INV2	x		x		x		✓	INV3	x		x		x	
1275-B-3	F	INV2	x		✓	INV3	✓	INV2	x		x		x		✓	INV3	x		x		x	
2476-1-4	F	INV2	x		✓	INV3	✓	INV2	x		x		x		✓	INV3	x		x		x	
2484-1-1	F	INV2	x		x		x		x		x		x		✓	INV2	x		x		x	
2962-2-1	M	INV2	x		x		x		x		x		x		✓	INV2	x		x		x	
2513-1-4	M	INV2	x		✓	INV3	✓	INV2	x		x		x		✓	INV3	x		x		x	
3121-1-4	F	INV2	x		x		✓	INV2	x		x		x		x		x		x		x	
3084-1-1	M	INV2	x		✓	INV3	✓	INV2	x		x		x		✓	INV3	x		x		x	
3158-4-1	F	INV2	x		✓	INV3	✓	INV2	x		x		x		✓	INV3	x		x		x	
3182-1-2	F	INV2	x		✓	INV3	✓	INV2	x		x		x		✓	INV3	x		x		x	
3183-1-4	F	INV2	x		✓	INV3	✓	INV2	x		x		x		✓	INV3	x		x		x	
3234-1-4	M	INV2	x		✓	INV3	✓	INV2	x		x		x		✓	INV3	x		x		x	
Total # of lines tested per assay			13		29		40		13		4		13		31		13		2		6	

INV, investigator 1-4, N/A, not applicable, check marks represent completed experiments, x marks represent experiment that have not performed.

Table S3 | qRT-PCR primer sequences.

GAPDH	Forward	AGGGCTGCTTTTAACTCTGGT
	Reverse	CCCCACTTGATTTTGGAGGGA
β-ACTIN	Forward	TGTCCCCCAACTTGAGATGT
	Reverse	TGTGCACTTTTATTCAACTGGTC
GFAP	Forward	GTCCCCCACCTAGTTTGCAG
	Reverse	TAGTCGTTGGCTTCGTGCTT
S100β	Forward	TGTAGACCCTAACCCGGAGG
	Reverse	TGCATGGATGAGGAACGCAT
VIM	Forward	TGGACCAGCTAACCAACGAC
	Reverse	GCCAGAGACGCATTGTCAAC
AQP4	Forward	GGCCGTAATCTGACTCCCAG
	Reverse	TGTGGGTCTGTCACTCATGC
ACSBG1	Forward	CCCCTTGACCTGTGATGACC
	Reverse	GAGACGGGATGGACTTGGA
APOE	Forward	GAGCAGGCCCAGCAGATAC
	Reverse	CTGCATGTCTTCCACCAGGG
βIII-TUBULIN	Forward	CCCGTTATCCCAGCTCCAATATGCT
	Reverse	ATGGCTTGACGTGCGTACTTCTCC
MAP2AB	Forward	AAACTGCTCTTCCGCTCAGACACC
	Reverse	GTTCACTTGGGCAGGTCTCCACAA
RELN	Forward	CATGATCAATGGGCTTTGGAC
	Reverse	GTATCGCCTAAGTGACCTTCG
CACNA1C	Forward	GAAGCGACAGAAGGACCG
	Reverse	CAAAAGGCCTAGGGAATGAGG

Table S4 | Genes included in the microfluidic cards.

Gene Symbol	Gene name	LifeTechnologies assay ID	RefSeq ID	Unigene ID
GAPDH	glyceraldehyde-3-phosphate dehydrogenase	Hs02758991_g1	NM_001256799.1	Hs.544577
18s RNA	eukaryotic 18s rRNA	Hs99999901_s1	NR_003286.2	-
SOX2	SRY (sex-determining region-Y)-box 2	Hs01053049_s1	NM_003106.3	Hs.518438
POU5F1	POU class 5 homeobox 1	Hs00999632_g1	NM_001173531.1	Hs.249184
LIN28A	lin-28 homolog A (C.elegans)	Hs00702808_s1	NM_024674.4	Hs.86154
NANOG	nanog homeobox	Hs04399610_g1	NM_024865.2	Hs.635882
NES	nestin	Hs04187831_g1	NM_006617.1	Hs.527971
FN1	fibronectin 1	Hs01549976_m1	NM_002026.2	Hs.203717
TUBB3	tubulin, beta 3 class III	Hs00801390_s1	NM_001197181.1	Hs.511743
FOXA2	forkhead box A2	Hs00232764_m1	NM_021784.4	Hs.155651
PAX6	paired box 6	Hs00240871_m1	NM_000280.4	Hs.270303
MAP2	microtubule-associated protein 2	Hs00258900_m1	NM_001039538.1	Hs.368281
RELN	reelin	Hs01022607_m1	NM_005045.3	Hs.655654
RBFOX3	RNA binding protein, fox-1 homolog (C.elegans) 3	Hs01370653_m1	NM_001082575.1	Hs.135229
ENO2	enolase 2 (gamma, neuronal)	Hs00157360_m1	NM_001975.2	Hs.511915
DLG4	discs, large homolog 4 (Drosophila)	Hs00176354_m1	NM_001128827.1	Hs.463928
CACNA1C	calcium channel, voltage-dependent, L-type, alpha 1C subunit	Hs00167681_m1	NM_000719.6	Hs.118262
GFAP	glial fibrillary acidic protein	Hs00909233_m1	NM_001131019.2	Hs.514227
VIM	vimentin	Hs00958111_m1	NM_003380.3	Hs.455493
S100B	s100 calcium binding protein B	Hs00902901_m1	NM_006272.2	Hs.422181
ALDH1L1	aldehyde dehydrogenase 1 family, member L1	Hs00201836_m1	NM_001270364.1	Hs.434435
ALDOC	aldolase C, fructose-biphosphate	Hs00902799_g1	NM_005165.2	Hs.155247
AIF1	allograft inflammatory factor 1	Hs00610419_g1	NM_001623.3	Hs.76364
ITGAM	integrin, alpha M (complement component 3 receptor 3 subunit)	Hs00355885_m1	NM_000632.3	Hs.172631

Table S5 | Proteome Profiler Human Cytokine Array.

Gene Symbol	Description
C5	Complement component 5
CD40LG	CD40 ligand
G-CSF	Granulocyte-colony stimulating factor
GM-CSF	Granulocyte-macrophage colony-stimulating factor
CCL1	Chemokine (C-C motif) ligand 1
CCL2/MCP-1	Chemokine (C-C motif) ligand 2
CCL3/MIP-1 alpha	Chemokine (C-C motif) ligand 3
CCL5/RANTES	Chemokine (C-C motif) ligand 5
CXCL1	Chemokine (C-X-C motif) ligand 1 (melanoma growth stimulating activity, alpha)
CXCL10/IP-10	Chemokine (C-X-C motif) ligand 10
CXCL11/I-TAC	Chemokine (C-X-C motif) ligand 11
CXCL12/SDF-1	Chemokine (C-X-C motif) ligand 12
ICAM-1	Intercellular Adhesion Molecule 1
IFN-gamma	Interferon, gamma
IL-1α	Interleukin 1 alpha
IL-1β	Interleukin 1 beta
IL-1ra	Interleukin 1 receptor antagonist
IL-2	Interleukin 2
IL-4	Interleukin 4
IL-5	Interleukin 5
IL-6	Interleukin 6
IL-8	Interleukin 8
IL-10	Interleukin 10
IL-12 p70	Interleukin 12
IL-13	Interleukin 13
IL-16	Interleukin 16
IL-17	Interleukin 17
IL-17E	Interleukin 17E
IL-18	Interleukin 18
IL-21	Interleukin 21
IL-27	Interleukin 27
IL-32α	Interleukin 32 alpha
MIF	Macrophage migration inhibitory factor (glycosylation-inhibiting factor)
Serpin E1/PAI-1	Serpin Family E Member 1/Plasminogen activator inhibitor-1
TNF-α	Tumor necrosis factor-alpha
TREM-1	Triggering receptor expressed on myeloid cells 1

SUPPLEMENTAL EXPERIMENTAL PROCEDURES

NPC-Astrocyte differentiation and culture

Forebrain NPCs were maintained at high density, grown on matrigel (BD Bioscience) in NPC medium (DMEM/F12 (Invitrogen: 10565), 1x N2 (Invitrogen: 17502-048), 1x B27-RA (Invitrogen: 12587-010)) and 20 ng/ml FGF2 (Invitrogen), resuspended in 1% BSA (Gibco) in PBS (Gibco)) and split approximately 1:3 every week with accutase (Millipore). NPCs could be expanded up to 14 passages. The quality of NPCs used for astrocyte differentiation is a critical variable in this protocol; careful quality control of NPC fate will increase the likelihood of a successful astrocyte differentiation. Low passage NPCs are frequently preferable. The astrocyte differentiation propensity of particularly intransient NPC lines can be improved by sorting for a CD271-/CD133+/CD184+ population by FACS (Cheng et al., 2017).

Forebrain NPCs were differentiated to astrocytes by seeding dissociated single cells at 15,000 cells/cm^2 density on matrigel-coated plates in astrocyte medium (ScienCell: 1801, astrocyte medium (1801-b), 2% fetal bovine serum (0010), astrocyte growth supplement (1852) and 10U/ml penicillin/streptomycin solution (0503)). Initial NPC seeding density and single cell dissociation are critical, particularly during the first 30 days of differentiation, in order to efficiently generate a homogenous population of astrocytes.

At day -1, after 5-10 min incubation with accutase at 37°C, NPCs were pipetted with a p1000 pipette 3-5 times, in order to yield a single cell suspension but limit cell death. Additional NPC medium was added and cells were transferred to a 15ml tube, spun at 500g for 5min, and plated on a matrigel-coated plate in NPC medium. At day 0, NPC medium was switched to astrocyte medium. From day 2, cells were fed every 48 hours for 20-30 days. When the cells reached 90-95% confluency (approximately every 6-7 days), they were split to the initial seeding density (15,000 cells/cm^2) as single cells in astrocyte medium, and cultured on matrigel, following 5-10 min incubation with accutase, pipetting, and washing with DMEM (Gibco).

After 30 days of differentiation, astrocytes could be split 1:3 every week with accutase and expanded up to 120 days (15-17 passages) in astrocyte medium containing 2% FBS. Following the initial 30-day differentiation period, astrocytes survive and expand for up to 30 days without FBS. All cell lines in the manuscript routinely tested negative for mycoplasma with MycoAlert PLUS mycoplasma detection kit (Lonza).

We caution that morphology and functional properties of hiPSC-astrocytes can change with increased passage (data not shown), which should be carefully recorded and matched in all experimental comparisons.

NPC differentiation from human iPSCs

hiPSCs were maintained in Human Embryonic Stem cell (HuES) medium (DMEM/F12 (Invitrogen), 20% KO-Serum Replacement (Invitrogen), 1x Glutamax (Invitrogen), 1x NEAA (Invitrogen), 1x 2-mercaptoethanol (Gibco), or complete mTeSR1 (StemCell Technologies) with 10 ng/ml StemBeads FGF2 (StemCultures) and differentiated to NPCs by either: 1) dual SMAD inhibition (0.1μM LDN193189 and 10μM SB431542) (Brennand et al., 2011) during embryoid body (EB) and rosette formation in EB medium (DMEM/F12 (Invitrogen: 10565), 1x N2 (Invitrogen: 17502-048), 1x B27-RA (Invitrogen: 12587-010)) or 2) Neural Induction Medium (StemCell Technologies). Rosette selection was performed after 14 days of culture by Rosette Selection Reagent (StemCell Technologies). NPCs were validated immunocytochemically

and/or by FACS using markers for SOX2 (Cell signaling: 3579S), PAX6 (Abcam: ab5790), FOXP2 (Abcam: ab16046) and NESTIN (Abcam: ab22035).

Generation of iNeurons from Human NPCs

NPCs were dissociated with accutase (Innovative Cell Technologies) and plated at 500,000 cells per well of a 24-well plate on day -2. Cells were plated on matrigel (BD Biosciences)-coated coverslips or plates in NPC medium (DMEM/F12/N2/B27/FGF2, Invitrogen). On day -1, h*NGN2* lentivirus (TetO-h*NGN2*-P2A-PuroR (Addgene: 79049) or TetO-h*NGN2*-P2A-eGFP-T2A-PuroR (Addgene: 79823)) together with CAGGs-rtTA lentivirus(Ho et al., 2015) at $1x10^6$ pfu/ml per plasmid (multiplicity of infection (MOI) of 2) was added in fresh NPC medium and spinfected at 1,000g for 1 hours. After 3-4 hours, the medium was replaced with fresh NPC medium. Doxycycline (2μg/l, Clontech) was added on day 0 to induce TetO gene expression and retained in the medium until the end of the experiment. On day 1, a 48 hr puromycin selection (1 μg/ml) period was started. On day 2, the culture medium was replaced by neuron medium: DMEM/F12 medium supplemented with N2/B27/Glutamax (Invitrogen) containing BDNF (20ng/ml, Peprotech), GDNF (10ng/ml, PeproTech), Dibutyryl cyclic-AMP (250μg/ml, Sigma), and L-ascorbic acid (200nM Sigma); Ara-C (2μg/l, Sigma) was added for 48 hours to the medium to inhibit proliferation of any non-neuronal cells. On day 4, hiPSC-derived astrocytes or primary astrocytes were seeded at 50,000 cells per well of the 24-well plate in the neuronal medium. FBS (2%) (Invitrogen) was added to the culture medium to support astrocyte viability. Beginning at day 4, half of the medium in each well was replaced every other day. h*NGN2*-induced neurons were assayed on day 17.

Flow Cytometry

Cells were dissociated using TryPLE (Gibco) or accutase (Millipore), fixed for 10 min in 4% paraformaldehyde (PFA), permeabilized and blocked with 0.5% (v/v) Triton (Sigma)/1% (w/v) bovine serum albumin (BSA, Sigma) in PBS and labeled with primary antibodies S100β (mouse, 1:200-1:1,000; Sigma-Aldrich: S2532), GFAP (chicken, 1:200-1:1,000; Aves Lab), GLAST/EAAT1 (rabbit, 1:100; BOSTER: PA2185), PAX6 (rabbit, 1:200; Abcam: ab5790), and NESTIN (mouse, 1:200; Abcam: ab22035) overnight at 4°C. Following 2 washes with 1 x PBS, the cell pellet was resuspended in blocking buffer with the appropriate Alexa Fluor 488, 568, or 647 conjugated secondary antibodies (1:200-1:1,000, Life Technologies) for 2hr at 4°C, then washed twice more with 1 x PBS, resuspended in FACS buffer (1 x PBS (no Mg2+/Ca2+)) and filtered using a 40 μm filter (BD Biosciences). Cytometry was performed using an LSR-II (BD Biosciences) and analysis was performed using Flowjo (v8.7.3, Treestar) or FCS Express 5 software (De Novo Software). Gating for positive cells was relative to a secondary antibody only control.

Immunocytochemistry

Cells were plated on acid-etched coverslips at 80,000-100,000 cells per well of a 24-well plate. Within 24hrs, astrocyte cultures were washed with PBS and fixed using 4% PFA (#15714, Electron Microscopy Sciences) for 20 min on ice, or 10% formalin solution (Sigma-Aldrich) for 15 minutes; washed 3 times with PBS 1X plus 0.01% Triton X-100 prior to pre-incubation with blocking solution made of PBS 1X plus 0.01% Triton X-100, and either 10% donkey serum or 1% bovine serum albumin (Sigma-Aldrich), for at least 1 hr. Cultures were then incubated in primary antibody solution overnight at 4˚C, followed by an incubation with secondary antibodies for 1-2hrs at room temperature. Primary antibodies used in this study were S100β (mouse, 1:1000; Sigma-Aldrich: S2532), GFAP (chicken, 1:2000; Aves Lab), Vimentin (rabbit, 1:500; Cell Signaling: R28#3932), b-III-tubulin (rabbit, 1:1000; Biolegend: 802001), polyclonal GLT1/EAAT2 and GLAST/EAAT1 (rabbit, 1:120, Life technology: PA5-34198), GLAST/EAAT1 (rabbit, 1:100;

BOSTER: PA2185), ALDH1L1 (rabbit, 1:250; Abcam: ab190298) PAX6 (rabbit, 1:200; Abcam: ab5790) NESTIN (mouse, 1:500; Abcam: ab22035), and Myelin Basic Protein (rabbit, 1:1000; Abcam:ab40390). Secondary antibodies used were Alexa Fluor 488, 568, or 647 conjugated (1:300, Life Technologies). Cultures were counterstained using 4',6-diamidino-2-phenylindole (DAPI, 1:1000-1:5000; Invitrogen: D1306). AquaPolymount mounting solution (#18606-20, Polysciences Inc.) was used to mount on coverslips. Coverslips were imaged with either a Zeiss LSM 780 microscope or Leica DMIL LED Inverted Routine Fluorescence Microscope.

RNA Expression studies for Quantitative Real Time PCR (qRT-PCR) and RNAseq

Cells were plated at 1,000,000 cells per well of a 6-well plate. Within 24-48 hrs, astrocyte cultures were washed with PBS and lysed with RLT buffer (Qiagen, # 74106) or Qiazol reagent (Qiagen). The total RNA was extracted from 30-day differentiated astrocytes with RNeasy mini kit (Qiagen, # 74106) with on-column DNaseI digestion (Qiagen, #79254) For standard qPCR, RNA was reverse transcribed into complementary DNA (cDNA) with iScript™ cDNA Synthesis kit (#1708890, Bio-Rad). cDNA was used as template for the quantitative PCR using a 7900 Real-Time PCR system (Applied Biosystems) with Power SYBR Green PCR Master Mix (Applied Biosystems). Gene expression was analyzed using the ΔΔCt method. qPCR results were normalized to GAPDH, β-actin and TBP (TATA-box binding protein) expression, and the values of uninduced fibroblasts were set to 1. Three replicates were used to determine the standard error. See the **Supplementary Table 3** for primer sequences.

For microfluidic card assays, RNA was reverse transcribed using the high capacity RNA to cDNA kit (LifeTechnologies). Individual channels on the cards were loaded with cDNA and Taqman® Universal Master Mix II (LifeTechnologies). The Taqman assays included in the microfluidic cards are listed in **Supplementary Table 4**. Gene expression was analyzed using the ΔΔCt method, and results were normalized to GAPDH and 18S ribosomal RNA. Gene expression fold changes were calculated compared to GAPDH expression. Each reaction was carried out in duplicate. The resulting data was subject to classical multidimensional scaling based on Euclidean distance in two dimensions, using R Studio (http://www.rstudio.com/). For RNAseq, RNA was quality controlled by BioAnalyzer (Agilent Technologies).

Analysis of RNA Sequencing Data

Paired-end RNA-seq data was generated using the Illumina HiSeq 2500 platform for hiPSC-astrocytes (n=4), neurons (n=6) and NPCs (n=8) (**Supplementary Table 5**), as well as for two primary astrocyte samples. Total RNA extracted from these samples was validated by qRT-PCR analysis before RNA sequencing. The paired-end sequencing reads were aligned to human hg19 genome using Star Aligner (version 2.5.0b). Following read alignment, FeatureCounts(Liao et al., 2014) was used to quantify gene expression at the gene level based on Ensembl gene model GRCh37.70. The gene level read counts data was normalized as counts per million (CPM) using the trimmed mean of M-values normalization (TMM) method(Robinson et al., 2010) to adjust for sequencing library size difference. To control for potential sex differences in gene expression, sex effects were corrected by linear regression. Multi-dimensional scaling (MDS) and cluster analysis were performed using the R programming language. Differential gene expression between different cell types was predicted by linear model analysis using the Bioconductor package limma(Ritchie et al., 2015). For differential expression between hiPSC-derived astrocytes and NPCs/neurons, a paired comparison was performed to account for matched genotypes. To adjust for multiple tests, the false discovery rate (FDR) of the differential expression test was estimated using the Benjamini–Hochberg (BH) method(Vasudevan et al.)·(Benjamini and Hochberg, 1995). Genes with FDR < 0.05 and log2 fold change > 1 or < -1 were considered significant.

Meta-analysis of brain cell type specific RNAseq data from Zhang *et al* 2016
We downloaded the raw RNAseq data of multiple brain cell types(Zhang et al., 2016) from gene expression omnibus (accession GSE73721) and then processed the sequencing reads using the same star-FeatureCounts pipeline as described above. The gene level read counts were combined with the data generated in this project. The merged data was normalized using the TMM approach and then corrected for sex and batch using linear regression. Hierarchical cluster analysis was performed using R.

Functional enrichment analysis
For functional enrichment analysis of differential expression gene signatures, the gene ontology (GO) annotations, and canonical pathways (Biocarta, KEGG and Reactome) gene sets were obtained from the Molecular Signatures Database (MSigDB) v4.0(Subramanian et al., 2005). Enrichment analysis was carried out using the Fisher's exact test assuming the sets of genes were identically independently sampled from the genome-wide genes profiled. The BH approach was employed to constrain the FDR.

IL-6 ELISA, Multi-Analyte ELISArray and protein array
hiPSC-derived astrocytes and primary human fetal astrocytes were seeded at 200,000viable cells per well of a 24-well plate in astrocyte medium one day before the experiment. Cells were treated for 24 hours with 50 ng/ml or 100 ng/ml of Poly(I:C) (InvivoGen, #tlrl-pic), 10 µg/ml or 50 µg/ml of Lipopolysachharide (LPS) (Sigma-Aldrich, #L5886), or 5 μM or 10 μM of human beta amyloid, Aβ42 (CaliforniaPeptide, #641-15) and vehicle control solutions (Saline for Poly(I:C) and LPS or Tris-HCl, pH 7.5 for Aβ42). The medium from astrocyte-enriched cultures was collected, centrifuged at 21,000g for 5 min at 4˚C and stored at -20˚C or proceeded assays.

Samples from all experiments were processed in parallel; comparisons were made within ELISA plates but not between them. Samples were analyzed with an IL-6 ELISA assay (Affymetrix eBioscience, #88-7066) and Human Inflammatory Cytokines Multi-Analyte ELISArray (Qiagen, #MEH-004A), according to manufacturer's guidelines. Absorbance at 450 nm was measured by spectrophotometry and was quantified at 450 nm, using 570 nm as a reference wavelength. Gene expression profiles were analyzed by RT2 Profiler PCR Arrays (Qiagen). Proteome Profiler™ Human Cytokine Array (R&D Systems, #ARY005B) was used according to manufacturer's guidelines. Proteome profiler intensity dot blots were quantified using Gimp2.8 software and were normalized to mean intensities of reference spots.

Phagocytosis assay
BV2 mouse microglial cell line was maintained in DMEM (Gibco, 11965) supplemented with 5% FBS (Sigma, F4135) and 1:100 Pen Strep (Gibco, 15140). To analyze the influence of astrocyte-secreted factors on the phagocytic activity of BV2 microglia, hiPSC-derived astrocytes and primary human fetal astrocytes were plated at approximately 1 million cells per well in a 6-well plate and allowed to grow for 2 weeks prior to medium conditioning. Astrocyte conditioned medium (ACM) was collected after 2 days of incubation and centrifuged at 21,000g for 5min at 4 ˚C. BV2 cells were seeded at 200,000 cells per well in a 24-well plate and allowed to attach for 8 to 9 hours. Cells were washed once with PBS and treated with ACM from hiPSC-derived astrocyte and primary astrocyte cultures. BV2 cells incubated with fresh astrocyte medium were used as a control. Zymosan conjugated with a pHrodo red dye (Thermo Fisher, P35364) was dissolved in PBS at 1 mg/ml and sonicated for 10 minutes. After 20 hours of incubation with ACM, BV2 cells were washed with PBS once and further incubated with 30 µg of pHrodo-labeled for 3 hours. Cells were trypsinized, washed with PBS once and resuspended in 500 µl of 1% BSA in PBS. Cells were kept on ice and immediately analyzed by flow cytometry.

To analyze the phagocytic ability of hiPSC-derived astrocytes and primary astrocytes in comparison with BV2, cells were seeded at 120,000 cells per well in a 24-well plate and allowed to reach confluency. Cells were incubated with 20 μg of pHrodo-labeled myelin for 3 hours. Myelin was prepared from the wild type mouse brain as described in(Jahn et al., 2008), and labeled with red pHrodo dye according to the manufacturer's instructions (Thermo Fisher, P36600). After incubation cells were gently collected in accutase, washed with PBS and resuspended in 1% BSA in PBS. Uptake of pHrodo was immediately analyzed with flow cytometry.

To analyze the effect of astrocyte co-culture on the phagocytic ability of BV2 cells, hiPSC-derived astrocytes and primary astrocytes were seeded at 120,000 cells per well in a 24-well plate. Cells were allowed to reach confluency, when BV2 cells were seeded on top of astrocytes at 150,000 cells per well. After 24 hours the co-culture was treated with 30 μg of pHrodo-labeled zymosan for 3 hours, and collected in 1% BSA in PBS as described before for immediate analysis by flow cytometry.

For the analysis of cell populations in co-culture and their contribution to phagocytosis, incubation with pHrodo-labeled zymosan was followed by sample collection with trypsinization and further blocking in 2% BSA in PBS for 30 minutes on ice. Cells were surface-labeled with CD11b-APC (eBiosciences) 1:100 in 1% BSA in PBS for 1 hour on ice. For intracellular labeling cells were washed and fixed with 2% paraformaldehyde for 30 minutes on ice, then washed with PBS once and incubated with GFAP antibody 1:100 for 1 hour on ice. After a wash in PBS, cells were incubated with the secondary antibody 1:100 conjugated to AlexaFluor488 for 30 minutes on ice and prepared for flow cytometry analysis by a wash in PBS and resuspension in 1% BSA in PBS. At least 30,000 events were collected in each flow cytometry analysis. Cells were gated on an FSC-A / SSC-A dot plot to exclude cell debris, additional gating on an FSC-A / FSC-W dot plot was used to exclude doublets. Isotype control and secondary antibody only labeling were used to define the gates for cells positive for CD11b or GFAP labeling. Single labeling of co-cultured cells with pHrodo-labeled zymosan, CD11b-APC and GFAP were used to set up compensation between channels. Cells pre-treated with 2μM Cytochalasin D for 30 minutes before and during the incubation with pHrodo-labeled zymosan were used as a negative control for phagocytic ability of BV2 and to define the population of phagocytosing cells.

All flow cytometry data were acquired on a LSRII (BD Biosciences) and analyzed using FCS Express 5 software (De Novo Software). Phagocytic index was calculated for pHrodo+ population as follows: % of gated cells was multiplied by geometric mean fluorescence intensity of pHrodo and then divided by 10^6 for presentation.

Spontaneous calcium transient imaging

Calcium imaging analysis was performed on hiPSC-derived astrocytes or human primary astrocytes from cerebral cortex region (ScienCell) on acid-etched glass coverslips. Cells were incubated for 15 min at room temperature with 2 μM Fluo-4-AM (Invitrogen, F-14201) and 0.02% Pluronic F127 in Krebs HEPES buffer (KHB) (10 mM HEPES, 4.2 mM $NaHCO_3$, 10 mM dextrose, 1.18 mM $MgCl_2.6H_2O$, 1.18 mM $KH2PO_4$, 4.69 mM KCl, 118 mM NaCl, 1.29 mM $CaCl_2$, pH7.3), then washed three times with KHB and allowed to recover for 5 minutes in KHB. Time-lapse images (40x water-immersion objective; NA = 0.8) were acquired on the green channel (DM:485; BA:495-540HQ) at 1.16 s intervals (0.9 Hz) on an Olympus FV1000 MPE Microscope using a 473 nm laser (Olympus LD473nm (15mW)). Cells were imaged for 348 s under continuous perfusion with gravity-fed KHB. A single glutamate (3 μM) in KHB pulse was applied for 35 s beginning at ~ 35 s. We imaged an area of 380 μm^2 for multiple coverslips originating from 4 different hiPSC-astrocyte lines and 3 different primary astrocytes

preparations. For peak analysis, ROIs were first identified by automated segmentation of time-averaged images of image stacks using FluoroSNNAP (Patel et al., 2015) Fluorescence signal from the identified ROIs was then quantified by calculating mean pixel intensity values on the same program. Fluorescent traces were exported and then analyzed with custom Matlab routines that calculated the number and amplitude of Ca^{2+} spikes and percentage of spontaneously active cells. In peak detection, 50 RFU was taken as the minimum amplitude for a peak based on visual inspection of multiple recordings.

Statistical analysis

For all experiments, data are represented as mean ± SD or SEM of three to five biological replicates. Statistical significance was determined using a two-tailed homoscedastic Student's t-test or one-way ANOVA and Dunnett's post-hoc test for differences of means between each group and a control group of data with parametric distribution. Significant comparisons are labeled with * $p < 0.05$, ** $p < 0.01$, *** $p < 0.001$.

SUPPLEMENTAL REFERENCES

Benjamini, Y., and Hochberg, Y. (1995). Controlling the False Discovery Rate: A Practical and Powerful Approach to Multiple Testing. Journal of the Royal Statistical Society Series B (Methodological) *57*, 289-300.

Brennand, K.J., Simone, A., Jou, J., Gelboin-Burkhart, C., Tran, N., Sangar, S., Li, Y., Mu, Y., Chen, G., Yu, D*., et al.* (2011). Modelling schizophrenia using human induced pluripotent stem cells. Nature *473*, 221-225.

Cheng, C., Fass, D.M., Folz-Donahue, K., MacDonald, M.E., and Haggarty, S.J. (2017). Highly Expandable Human iPS Cell-Derived Neural Progenitor Cells (NPC) and Neurons for Central Nervous System Disease Modeling and High-Throughput Screening. Current protocols in human genetics *92*, 21 28 21-21 28 21.

Ho, S.M., Hartley, B.J., Tcw, J., Beaumont, M., Stafford, K., Slesinger, P.A., and Brennand, K.J. (2015). Rapid Ngn2-induction of excitatory neurons from hiPSC-derived neural progenitor cells. Methods.

Jahn, O., Tenzer, S., Bartsch, N., Patzig, J., and Werner, H.B. (2008). Myelin Proteome Analysis: Methods and Implications for the Myelin Cytoskeleton. Neuromethods *79*, 171–236.

Liao, Y., Smyth, G.K., and Shi, W. (2014). featureCounts: an efficient general purpose program for assigning sequence reads to genomic features. Bioinformatics *30*, 923-930.

Patel, T.P., Man, K., Firestein, B.L., and Meaney, D.F. (2015). Automated quantification of neuronal networks and single-cell calcium dynamics using calcium imaging. J Neurosci Methods *243*, 26-38.

Ritchie, M.E., Phipson, B., Wu, D., Hu, Y., Law, C.W., Shi, W., and Smyth, G.K. (2015). limma powers differential expression analyses for RNA-sequencing and microarray studies. Nucleic Acids Research *43*, e47.

Robinson, M.D., McCarthy, D.J., and Smyth, G.K. (2010). edgeR: a Bioconductor package for differential expression analysis of digital gene expression data. Bioinformatics *26*, 139-140.

Subramanian, A., Tamayo, P., Mootha, V.K., Mukherjee, S., Ebert, B.L., Gillette, M.A., Paulovich, A., Pomeroy, S.L., Golub, T.R., Lander, E.S*., et al.* (2005). Gene set enrichment analysis: A knowledge-based approach for interpreting genome-wide expression profiles. Proceedings of the National Academy of Sciences of the United States of America *102*, 15545-15550.

Vasudevan, B., Ashish, B., Amitabh, S., and A, P.M. (2010). Primary Cutaneous Histoplasmosis in a HIV-Positive Individual. Journal of global infectious diseases *2*, 112-115.

Zamanian, J.L., Xu, L., Foo, L.C., Nouri, N., Zhou, L., Giffard, R.G., and Barres, B.A. (2012). Genomic analysis of reactive astrogliosis. J Neurosci *32*, 6391-6410.

Zhang, Y., Sloan, S.A., Clarke, L.E., Caneda, C., Plaza, C.A., Blumenthal, P.D., Vogel, H., Steinberg, G.K., Edwards, M.S., Li, G*., et al.* (2016). Purification and Characterization of Progenitor and Mature Human Astrocytes Reveals Transcriptional and Functional Differences with Mouse. Neuron *89*, 37-53.